



Air-sea stability effects on the 10 m winds over the global ocean: Evaluations of air-sea flux algorithms

A. B. Kara,¹ A. J. Wallcraft,¹ and M. A. Bourassa²

Received 7 May 2007; revised 4 December 2007; accepted 3 January 2008; published 9 April 2008.

[1] Spatial and temporal variability of the impact of air-sea stratification on the differences between satellite-derived 10 m equivalent neutral wind speeds and stability-dependent (e.g., in situ) 10 m wind speeds are quantitatively examined over the global ocean. The influences of stability are compared with three air-sea flux algorithms, Coupled Ocean-Atmosphere Response Experiment (version 3.0), Bourassa-Vincent-Wood, and Liu-Katsaros-Businger. Analyses are first presented at many individual buoy locations and then are extended to the global ocean with the use of rain-free wind measurements from the SeaWinds scatterometer on the QuikSCAT satellite, gridded at a resolution of $0.25^\circ \times 0.25^\circ$. Overall, stability-dependent winds are found to be weaker than equivalent neutral winds by 0.2 m s^{-1} on the basis of 7619 monthly mean values from 208 buoys during 2000–2005. Differences based on hourly winds can be as large as $\pm 0.5 \text{ m s}^{-1}$. Results remain robust regardless of which air-sea flux algorithm is used. Monthly rain-free gridded QuikSCAT measurements, combined with atmospheric stability determined using near-surface variables from the European Centre for Medium-Range Weather Forecasts 40-year reanalysis, demonstrate the effects of stratification on the 10 m winds globally. Differences in stability-dependent and neutral winds are substantially nonsymmetrical and reveal locations where the former is stronger than the latter. These differences may cause physically significant biases in air-sea fluxes if they are not properly considered, especially near the Kuroshio and Gulf Stream current systems.

Citation: Kara, A. B., A. J. Wallcraft, and M. A. Bourassa (2008), Air-sea stability effects on the 10 m winds over the global ocean: Evaluations of air-sea flux algorithms, *J. Geophys. Res.*, 113, C04009, doi:10.1029/2007JC004324.

1. Introduction

[2] Accurate wind speeds are essential for reliable computations of surface heat and momentum fluxes (e.g., wind stress and sensible and latent heat fluxes) over the global ocean. The sampling density (particularly for data-sparse regions) and accuracy make satellite winds desirable data for many related applications such as coastal upwelling, oceanic/atmospheric coupling associated with both tropical instability wave and ocean fronts [Chelton *et al.*, 2004], ocean currents [Lagerloef *et al.*, 2003], and detection of tropical disturbances [Gierach *et al.*, 2007], to list a small sample of applications.

[3] Quantifying the effects of atmospheric stability on satellite-derived wind speed (called equivalent neutral wind speed) is a critical issue for various climate applications, where biases related to such processes would be of interest in flux calculations, product intercomparisons, and ocean model simulations. Of particular interest are scatterometers, spaceborne radars that infer surface winds from the rough-

ness of the ocean surface [Liu, 2002]. They respond to changes in the water surface rather than responding directly to wind speed.

[4] Surface roughness is more closely related to wind stress than to wind speed [Bourassa, 2006]. While this would seem ideal for ocean forcing, the scatterometer time series has existed for a relatively short time, and most ocean models are forced by stress determined from wind speed [e.g., Barron *et al.*, 2006]. Satellite winds (e.g., from scatterometers and radiometers) are well suited for such applications, provided that considerations such as ocean currents [Kara *et al.*, 2007a] and atmospheric stability [Kara *et al.*, 2005] are properly considered in the conversion of satellite winds to stresses. Satellite winds are calibrated such that these considerations have already been accounted for: further adjustments result in regional biases in surface forcing. Specifically, scatterometers and radiometers are calibrated to equivalent neutral wind speeds at 10 m above the ocean surface [e.g., Meissner *et al.*, 2001] rather than to wind speeds including effects of stratification. Hereinafter, the latter will be referred to as stability-dependent winds.

[5] The conversion of equivalent neutral wind speeds to stability-dependent ones is complicated by several definitions of the neutral wind as well as conflicting assumptions used to determine an equivalent neutral wind. In general, there are two definitions. In the most common definition,

¹Oceanography Division, Naval Research Laboratory, Stennis Space Center, Mississippi, USA.

²Center for Ocean-Atmospheric Prediction Studies and Department of Meteorology, Florida State University, Tallahassee, Florida, USA.

Table 1. List of Algorithms Used in This Paper^a

Abbreviation	Air-Sea Flux Algorithm	Reference
COARE	Coupled Ocean-Atmosphere Response Experiment	<i>Fairall et al.</i> [2003]
LKB	Liu-Katsaros-Businger model	<i>Liu and Tang</i> [1996]
BVW	Bourassa-Vincent-Wood model	<i>Bourassa et al.</i> [1999]
BVWN	Bourassa-Vincent-Wood neutral model	<i>Bourassa et al.</i> [1999]
LOG	Logarithmically varying profile	<i>Peixoto and Oort</i> [1992]

^aAbbreviations used throughout the paper are given. A brief description for each algorithm is provided in the text. For detailed descriptions, see references. The modern version of the LKB model [*Liu and Tang*, 1996] differs from the original algorithm in that it increases the momentum roughness length by adding roughness due to gravity wave via a Charnock parameterization.

equivalent neutral wind speed is the mean wind speed that would be observed if there was neutral atmospheric stratification [*Geernaert and Katsaros*, 1986]. This definition is useful for determining neutral drag coefficients and roughness lengths. However, this definition requires assumptions on what (if anything) is held constant, which may not be appropriate globally. The second definition [*Ross et al.*, 1985; *Liu and Tang*, 1996] of equivalent neutral wind is the wind speed calculated by using the stress and roughness length consistent with the observed atmospheric stratification but setting the atmospheric stratification term in the modified log-wind profile equal to zero. This definition may be more consistent with scatterometry, which measures surface stress [*Weissman et al.*, 1994]. Unfortunately, accurate measurements of near-surface stress over water are extremely sparse relative to wind speed. Another issue to consider is that scatterometer equivalent neutral winds are relative to current and are further modified by surface wave motion [*Bourassa*, 2006] from scatterometer winds. The considerations of wave motion and currents are physically important in the calculation of surface turbulent fluxes [e.g., *Kara et al.*, 2007a]. Herein, we focus on the impact of atmospheric stability.

[6] There are earlier studies related to satellite calibration/validation, which adjusted in situ observations to be physically consistent with equivalent neutral winds. For example, *Mears et al.* [2001] used Special Sensor Microwave Imager winds during 1987–1997, and *Ebuchi et al.* [2002] analyzed QuikSCAT winds during 1999–2000 at many individual buoy locations. *Bourassa et al.* [2003] evaluated SeaWinds data with research vessels. Each of these earlier studies adjusted the in situ observations to equivalent neutral winds. *Mears et al.* [2001] found that the distribution of adjustments had little dependence on the flux algorithm used for adjustment. However, they expressed this distribution through means and standard deviations. We will show that the distribution of adjustments is substantially non-Gaussian and that there can be large changes in the distribution if an overly simple adjustment algorithm is applied.

[7] In this paper, we focus on the distribution of such differences and examine the regional variability on a fine (relative to most global ocean models) grid resolution ($0.25^\circ \times 0.25^\circ$) over the global ocean during 2000–2005. This is accomplished by using a variety of air-sea flux algorithms. We quantify the difference between equivalent

neutral winds and those including influences of stratification to provide a comprehensive analysis over the global ocean. This is the first study demonstrating how the differences vary regionally and globally.

2. Air-Sea Flux Algorithms

[8] The World Meteorological Organization has defined 10 m as the reference height for near-surface wind observations. We will use various algorithms to adjust wind speed at an observed height (e.g., 4 m above the surface) to the standard height of 10 m. Each algorithm will be applied to observed winds, some of which include air-sea stratification effects and some of which do not.

[9] A list of algorithms used for adjusting observed winds to 10 m above the ocean surface and calculating equivalent neutral winds and stability-dependent winds is provided in Table 1 along with their abbreviations. The reason for using different algorithms is to investigate whether or not the resulting adjusted winds deviate significantly. These algorithms have been well described in the literature. Thus, only a brief description for each is provided. Further details can be found in references (see Table 1).

[10] The Coupled Ocean-Atmosphere Response Experiment (COARE version 3.0) and Bourassa-Vincent-Wood (BVW) algorithms will be used for obtaining height-adjusted stability-dependent 10 m winds (i.e., including stratification effects at the air-sea interface). The Liu-Katsaros-Businger (LKB), Bourassa-Vincent-Wood neutral (BVWN), and logarithmically varying profile (LOG) algorithms will be used for obtaining the 10 m equivalent neutral winds. Unlike the COARE algorithm, BVW has an option of calculating both equivalent neutral winds and winds based on the air-sea stability. All algorithms have advantages and disadvantages over each other because of their unique parameterizations [e.g., *Brunke et al.*, 2003], whose details are not given here.

[11] The COARE algorithm attempts to take full account of atmospheric stability in the near-surface layer. This is achieved by iteratively solving for the stability of the atmosphere. The algorithm uses the stable profile functions from *Beljaars and Holtslag* [1991] and the convective portion of the scalar profile function described by *Grachev et al.* [2000]. The threshold value $z/L = 1$, where z is the height above the ocean surface and L is the Monin-Obukhov length, for very stable cases, is not a strict limit in the algorithm. The use of the critical bulk Richardson number is more suitable to setting a very stable limit. A bulk Richardson number of about 0.2 is taken as the critical value [*Grachev et al.*, 2005]. There is no explicit option of the equivalent neutral winds in the algorithm.

[12] The BVW model is a fully coupled flux and ocean state model. Coupling allows the ocean state to respond to atmospheric stability and vice versa. The profile stability functions in the algorithm were obtained from *Beljaars and Holtslag* [1991] for stable conditions and from *Benoit* [1977] for unstable conditions. Typically, the parameterizations in BVW relate surface roughness lengths, and hence the exchange coefficients, to various aspects of sea state, swell, gravity waves, and capillary waves. It can provide both stability-dependent and equivalent neutral winds.

[13] LKB is also based on the similarity functions (i.e., nondimensional flux-profile relations) in the atmospheric

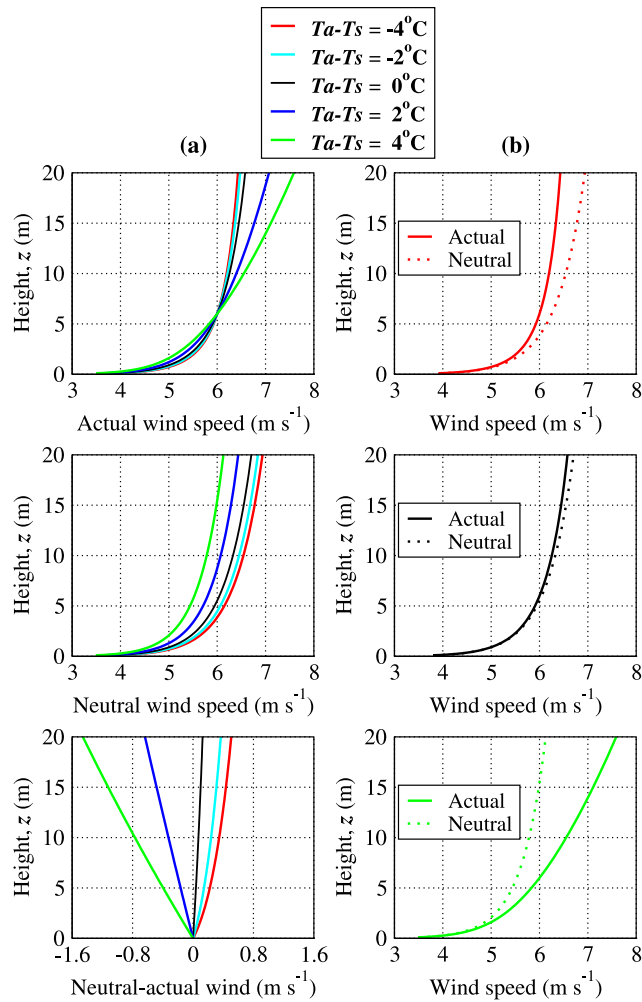


Figure 1. (a) Typical variations of (top) actual, i.e., stability-dependent, and (middle) equivalent neutral winds with height along with (bottom) the differences between the two. The black lines for stability-dependent and neutral winds are similar because they represent conditions near neutral atmospheric stratification. (b) Comparison of stability-dependent and neutral wind speeds for (top) unstable, (middle) neutral, and (bottom) stable conditions. Stable (unstable) stratification corresponds to positive (negative) air-sea temperature, and it reduces (increases) mixing through surface stress.

surface layer. As in COARE and BVW, bulk parameterizations are used for determining flux-profile relationships of heat and moisture within the surface layer. The interfacial effects within the molecular sublayer at the sea surface are included because it is assumed to be the most limiting (slowest) process. The wind profile in the sublayer profile is given an exponential shape. Theoretically, the validity of LKB depends on the validity of the modeled surface renewal and similarity theory. For example, when turbulence is suppressed by stable density stratification (bulk Richardson number exceeds a critical value), the results may not be valid and the algorithm may fail to converge.

[14] The LOG approach is the simplest one that is used for adjusting winds. Similar to LKB, it works for the equivalent neutral winds. Assuming a logarithmically vary-

ing wind profile, the corrected wind speed at a height z is given by $U_{\text{LOG}}(z) = \ln(z/z_o)/[\ln(z_m/z_o)]U(z_m)$. Here, z_o is the roughness length. The typical oceanic value for z_o is 1.52×10^{-4} m [Peixoto and Oort, 1992].

3. Definition of the Equivalent Neutral Wind

[15] The wind speed dependence on height is typically expressed as follows:

$$U(z) - U_s = (u^*/k)[\ln(z/z_o)] + (u^*/k)\Phi(z, z_o, L), \quad (1)$$

where term 1 ($U(z) - U_s$) denotes the wind speed relative to the surface speed U_s (e.g., the surface current) as a function of height z . In term 2 ($(u^*/k)[\ln(z/z_o)]$), the friction velocity (u^*) is the square root of the kinematic stress, and the von Kármán constant (k) has a value of 0.4. Term 2 is the adjustment for height that does not directly consider atmospheric stability; however, atmospheric stability enters indirectly through the friction velocity and roughness length. The quantity $\Phi(z, z_o)$ in term 3 ($(u^*/k)\Phi(z, z_o, L)$) denotes the direct modification due to atmospheric stratification based on the Obukhov scale length (L). Both u^* and z_o are functions of U_s , atmospheric stratification, and ocean state. When the atmospheric stratification is neutral (i.e., $z/L = 0$), there is no stratification, and therefore, the stability term is set to zero. Equivalent neutral winds are calculated without term 3; however, they use roughness length and friction velocity that are first determined with term 3 included.

[16] Following (1), we illustrate the influence of air-sea temperature contrasts on the wind profile for both winds, including the effects of stability and the corresponding equivalent neutral winds (Figure 1a). In the example, the wind speed is set to 6 m s^{-1} at a height of 6 m. The air-sea mixing ratio difference is taken as 3 g kg^{-1} over the same height range, causing the profile with a zero temperature difference to be slightly unstable.

[17] Equivalent neutral wind profiles given in Figure 1a are determined with the definition of Liu and Tang [1996]. Clearly, there are considerable differences between the two sets of profiles. The wind profile is equal to the equivalent neutral wind profile only for the case of neutral stratification. Typically, these differences are $<0.5 \text{ m s}^{-1}$; however, they can be very large for atmospheric stratifications that are far from neutral, as evident from Figure 1a (bottom).

[18] For stable atmospheric stratification (green and blue lines), equivalent neutral winds are relatively weaker than stability-dependent winds, and for unstable atmospheric stratification (red and cyan lines), equivalent neutral winds are stronger than stability-dependent winds. Near the surface (i.e., below the top of the boundary layer with increasing differences closer to the surface), the wind speed is typically weaker when the air is stable and stronger when the air is unstable (Figure 1b).

4. Buoy Data and Wind Speed Adjustment to 10 m

[19] We use buoy data from three sources: (1) the Tropical Atmosphere-Ocean (TAO)/Triangle Trans-Ocean Buoy Network (TRITON) array [McPhaden et al., 1998], (2) the Pilot Research Moored Array in the Tropical Atlantic

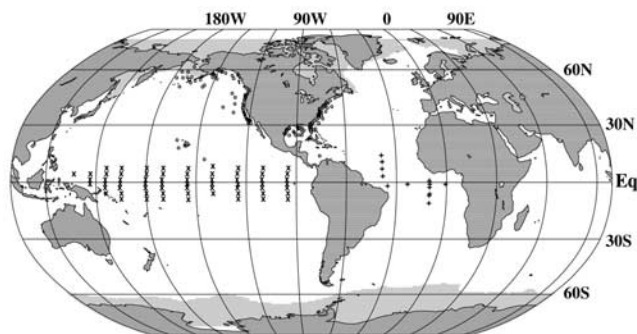


Figure 2. Locations of TAO (crosses), PIRATA (pluses), and NDBC (circles) buoys used in the analyses in this paper. The regions where ice exists are shown in gray. The wide distribution of the buoys and their records provides an ample source of data from which to test algorithms used in this paper in both open ocean (TAO and PIRATA buoys and some NDBC buoys) and coastal regions (most NDBC buoys) during long time periods.

(PIRATA) [Servain *et al.*, 1998], and (3) the National Data Buoy Center (NDBC) database, which is available from the National Oceanographic Data Center (<http://www.nodc.noaa.gov/BUOY/buoy.html>).

[20] Locations of buoys are shown in Figure 2. The heights of sensors at NDBC locations are generally the same, with values of 4 m for air temperature and humidity and 5 m for wind speed measurements. However, there are a few exceptions. For example, some NDBC buoys measure air temperature and wind speed at 3.2, 10.0, 12.3, and 13.8 m above the ocean surface. Both TAO and PIRATA buoys have identical measurement heights: air temperature and relative humidity are measured at 3 m above the ocean surface, and wind speed is measured at 4 m above the ocean surface. TRITON buoys in the Pacific west of 160°E measure winds at 3.5 m and measure relative humidity and air temperature at 2.2 m.

[21] Measurements of ocean surface temperature, air temperature, and relative humidity (or specific humidity) are used for adjusting winds to 10 m from their original heights and for calculating air-sea stability. Each buoy provides a time series of near-surface atmospheric variables, with the time period sampled in each record varying according to buoy deployment duration and sensor operation. We obtain time series of these historical atmospheric variables at hourly resolution from all available buoys from 2000 through 2005. There are 78 TAO, 117 NDBC, and 13 PIRATA buoys used in this study.

[22] For consistency at all TAO, NDBC, and PIRATA buoys, mixing ratio values for air (using air temperature) and ocean (using ocean surface temperature) are calculated using saturated vapor pressure. Air and ocean surface temperatures and ocean level pressures available at each location are used for computations. To calculate mixing ratio, dew point temperature is available from NDBC buoys, while TAO and PIRATA buoys provide relative humidity. TAO and PIRATA buoys do not generally measure atmospheric pressure; thus a constant value of 1013 mbar is used for density calculations.

[23] Positions of ocean buoys can change by up to ≈ 3 km over the course of a few days to a week depending on the

current regime. Since each mooring moves in time and space from its deployment position, we calculated average position on the basis of the historical latitude and longitude data for each buoy. For ease of notation, nearest integer values of average latitude and longitude are used for each buoy throughout the text.

[24] We first investigate how much wind speed changes when adjusting it to 10 m from a particular measurement height. All algorithms listed in Table 1 are modified (if needed) such that a measurement height for each buoy can be input for adjusting winds to 10 m as examined here or calculating equivalent neutral winds. Computations are performed on the basis of the available hourly buoy measurements, involving the above-mentioned near-surface atmospheric variables. The resulting winds are then averaged over a day and a month. We do not use buoy measurements for periods where any meteorological parameter required by the algorithms is missing, with the exception of pressure, which is set to 1013 mbar. Additionally, no averaging or smoothing is applied to the original parameters prior to using them in the algorithms. Daily and monthly means are then constructed to reduce data volume at all buoy locations.

[25] An example of the adjustment procedure is demonstrated at a TAO buoy, located at the equator (0°N, 155°W), in 2000 (Figure 3a). Wind speed measurements are made at a height of 4 m at this particular buoy location. As mentioned earlier, near-surface atmospheric variables are input to the COARE and BVW algorithms to adjust winds to a height of 10 m. The change in wind speed due to height adjustment is proportional to the observed wind speed. Therefore, the impact of adjustment for weaker winds (e.g., 3 m s^{-1}) is typically small in comparison to that for stronger winds (e.g., 8 m s^{-1}). For example, in the former (latter) case the 10 m wind is $\approx 0.3 \text{ m s}^{-1}$ ($\approx 0.8 \text{ m s}^{-1}$) stronger than the 4 m wind. Wind speed at the measurement height of 4 m has an annual mean value of 6.3 m s^{-1} , and wind speed adjusted to 10 m using either COARE or BVW has an identical mean value of 6.8 m s^{-1} in 2000. In general, both COARE and BVW give nearly identical results, as also evident in Figure 3b. Annual mean difference between wind speeds at 10 and those at 4 m is 0.5 m s^{-1} when using either COARE or BVW in adjusting winds.

5. Differences Between Neutral and Stability-Dependent Winds

5.1. Analyses at Buoy Locations

[26] After the winds are adjusted to 10 m, as explained in section 4, we now form a difference between stability-dependent and equivalent neutral winds. This is first done at the previously analyzed buoy location (0°N, 155°W) in 2000 and 2001 and then repeated at all available TAO, NDBC, and PIRATA buoys during all available time periods from 2000 through 2005.

[27] Equivalent neutral winds are calculated using BVWN, LKB, and LOG, as listed in Table 1. Stability-dependent winds are typically weaker than their counterpart neutral winds, which is consistent with the typically unstable stratification at this buoy (Figure 4). Neutral winds from BVWN and LKB are almost identical in these examples, while those from LOG are different and have much less variability on daily timescales in both years. A standard

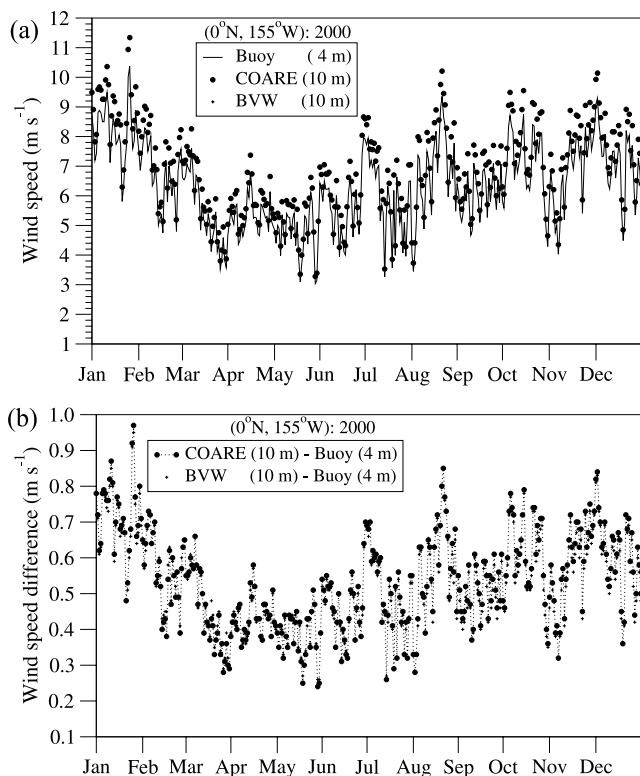


Figure 3. (a) Time series of daily averaged wind speed at 4 m above the sea surface as obtained from a TAO buoy, (0°N , 155°W), located in the central equatorial Pacific in 2000. Also given are wind speed values adjusted to 10 m using COARE (version 3.0) and BVW algorithms. (b) Differences between wind speeds adjusted to 10 m and those at 4 m. Symbols used for differences (circles and pluses) are generally overlain on each other for a given day, clearly confirming the fact that both algorithms give nearly identical results at this particular TAO buoy location. Note that the x axis is labeled starting from the beginning of each month.

LOG correction provides a neutral wind that is fairly consistently $<0.05 \text{ m s}^{-1}$ different from the stability-dependent wind.

[28] Hereinafter, BVW is used as a reference algorithm since it has an option of calculating either stability-dependent or equivalent neutral winds. Annual mean difference between the two is very small with values of -0.09 , -0.07 , and -0.04 m s^{-1} for BVW minus BVWN, BVW minus LKB, and BVW minus LOG, respectively, during 2000. The corresponding differences in 2001 are again small, with values of -0.13 , -0.11 , and -0.05 m s^{-1} . These differences (annual averages, averaged over all buoy locations) are small for most climate-related applications. They are substantially smaller than the accuracy of individual wind speed measurements, 0.3 m s^{-1} , at TAO buoys [Freitag *et al.*, 2001]; however, they are likely to be statistically significant. Regionally, the biases can be larger than 0.3 m s^{-1} .

[29] Similar to the TAO buoy location examined above, differences in stability-dependent and equivalent neutral winds are also analyzed at a NDBC location (29°N , 85°W). This buoy is west-northwest of Tampa, Florida,

United States, and water depth is $\approx 54 \text{ m}$. Winds at this particular buoy location are measured 5 m above the site level. Hourly measurements of near-surface variables are used for adjusting winds to 10 m with BVW, and for simplicity, the resulting winds are then averaged over a month (Figure 5). Also included are monthly averages of equivalent neutral winds computed with BVWN, LKB, and LOG algorithms to show differences among them. Results are given from 2000 through 2005 so that one could see interannual variations, given that wind speeds and stability can change depending on the time or the year. At this particular location, variations in wind speeds do exist from one year to another, but the common feature in all years is that winds during summer are typically weaker than those during other time periods.

[30] Differences between stability-dependent and equivalent neutral winds calculated with BVWN, LKB, and LOG are given in Figure 6 at (29°N , 85°W) during each year, separately. The most striking feature seen in Figure 6 is that the LOG algorithm is the outlier, as it generally yields neutral winds weaker than BVWN and LKB values. This difference in behavior is due to (1) the use of a neutral stress rather than the stability-dependent stress and (2) the fixed roughness length. The differences in neutral winds obtained from BVWN and LKB are relatively small. For example, the annual mean difference for BVW minus BVWN (BVW

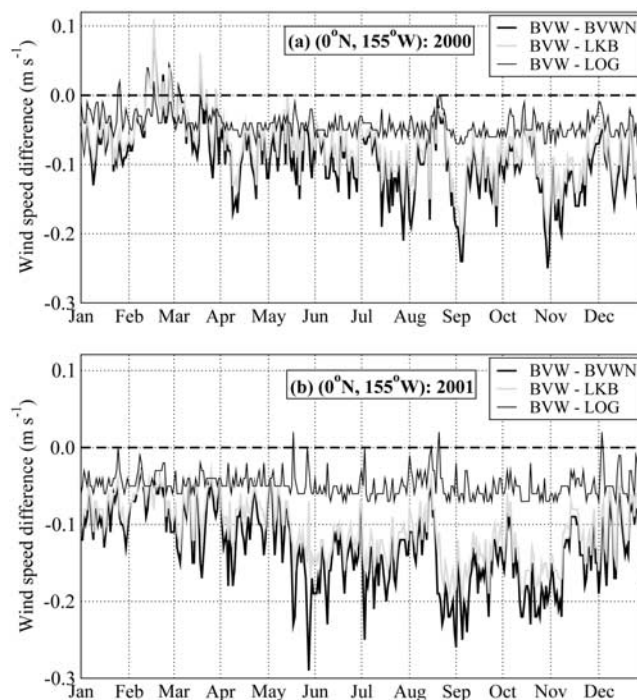


Figure 4. Differences in stability-dependent and equivalent neutral wind speeds at a TAO buoy, (0°N , 155°W). Comparisons are shown for (top) 2000 and (bottom) 2001. In all cases, stability-dependent wind speeds are adjusted to 10 m (from 4 m) by including the effects of stability using BVW, while equivalent neutral winds were adjusted to 10 m using BVWN, LKB, and LOG as described in the text. Note that unlike the others, the LOG approach, described in section 2, has no detailed physics in it and uses a constant roughness length.

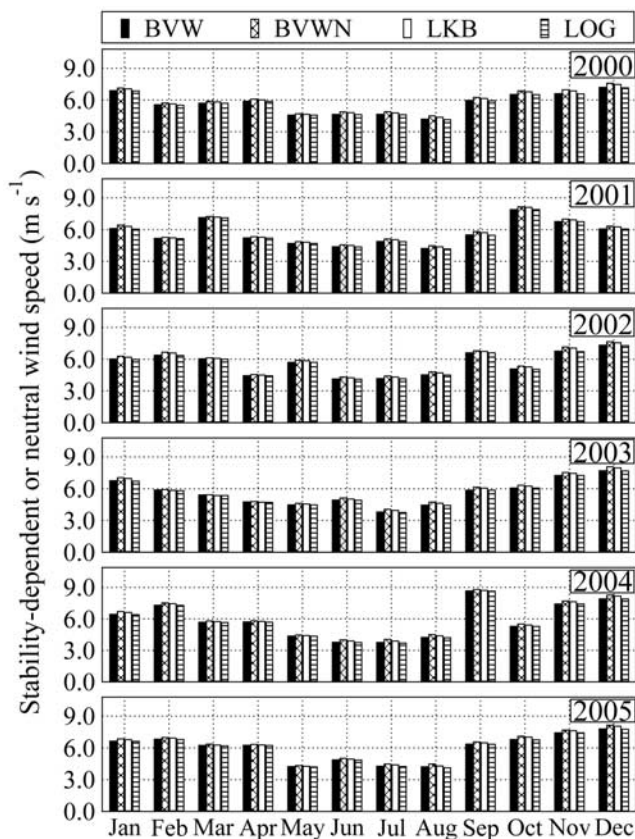


Figure 5. Monthly mean wind speeds at 10 m above the sea surface at a buoy location, (29°N, 85°W), whose NDBC station ID is 42036. Stability dependence in winds is taken into account using near-sea surface atmospheric variables in the BVW algorithm as described in the text. Equivalent neutral winds are computed with BVWN, LKB, and LOG algorithms. In all cases, individual hourly data are used to determine wind speeds and monthly means are then constructed.

minus LKB) is generally -0.2 m s^{-1} (-0.1 m s^{-1}) during most of the years from 2000 through 2005. On the basis of the LOG approach, stability-dependent winds are almost identical to equivalent neutral winds over the annual cycle. We cannot directly conclude which algorithm performs the best, but on the basis of these results it is clear that BVWN and LKB give comparable results.

[31] Monthly mean differences at the NDBC buoy location of (29°N, 85°W), shown in Figure 6, were computed on the basis of hourly wind speed measurements as mentioned above. We now produce a box plot to have a more qualitative analysis of hourly wind speed differences used for determining monthly mean among different algorithms. As an example, this is demonstrated in 2001 (Figure 7). The box plot simply summarizes hourly wind speed differences at the NDBC location. Each box contains the middle 50% (i.e., median) of the wind speed difference. The upper (lower) hinge of the box indicates the 95th (5th) percentile of the wind speed difference and is limited by the 5th percentile and 95th percentile differences, and the whiskers show the largest differences within the month. The median

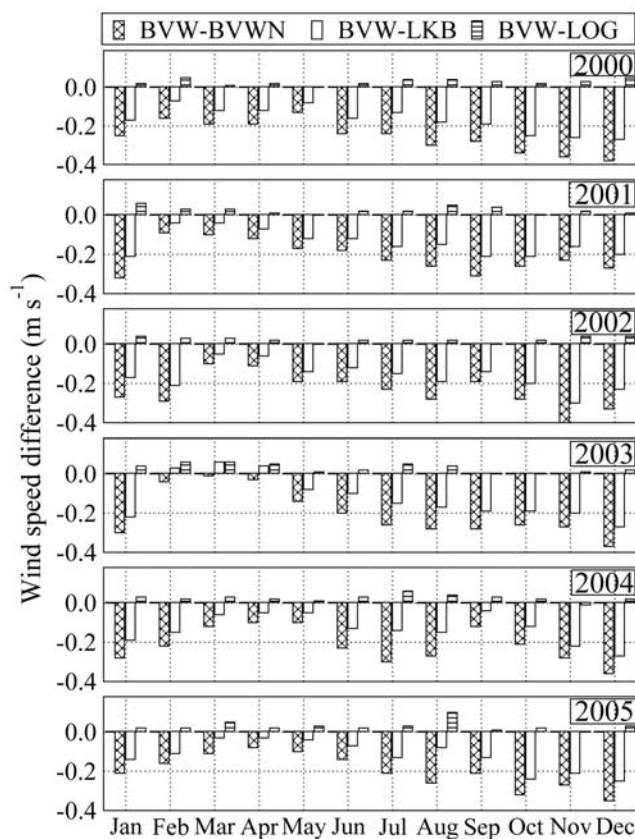


Figure 6. Differences between stability-dependent and equivalent monthly mean wind speeds at 10 m above the sea surface at (29°N, 85°W). Differences are based on values given in Figure 5.

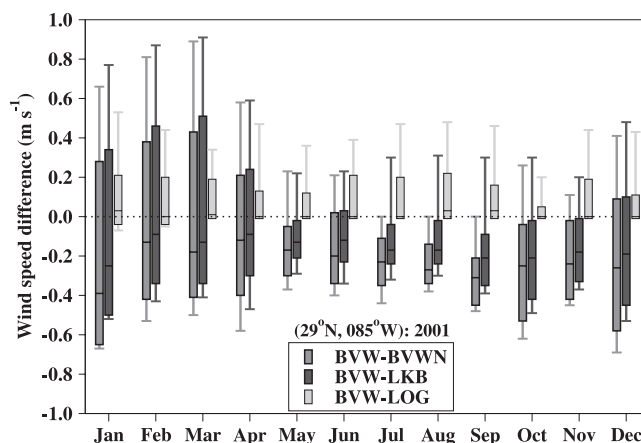


Figure 7. Box plots of differences between stability-dependent and equivalent neutral winds at (29°N, 85°W) in 2001. All these are calculated using hourly stability-dependent and neutral wind speeds for each month. For example, there are 743, 670, and 735 hourly wind speeds available from the buoy in January, February, and March, respectively. These winds are first adjusted to 10 m using the BVW algorithm. These 10 m winds are then converted to equivalent neutral winds using BVWN, LKB, and LOG. Differences from BVW are then computed to determine the statistical summary provided in the box plots.

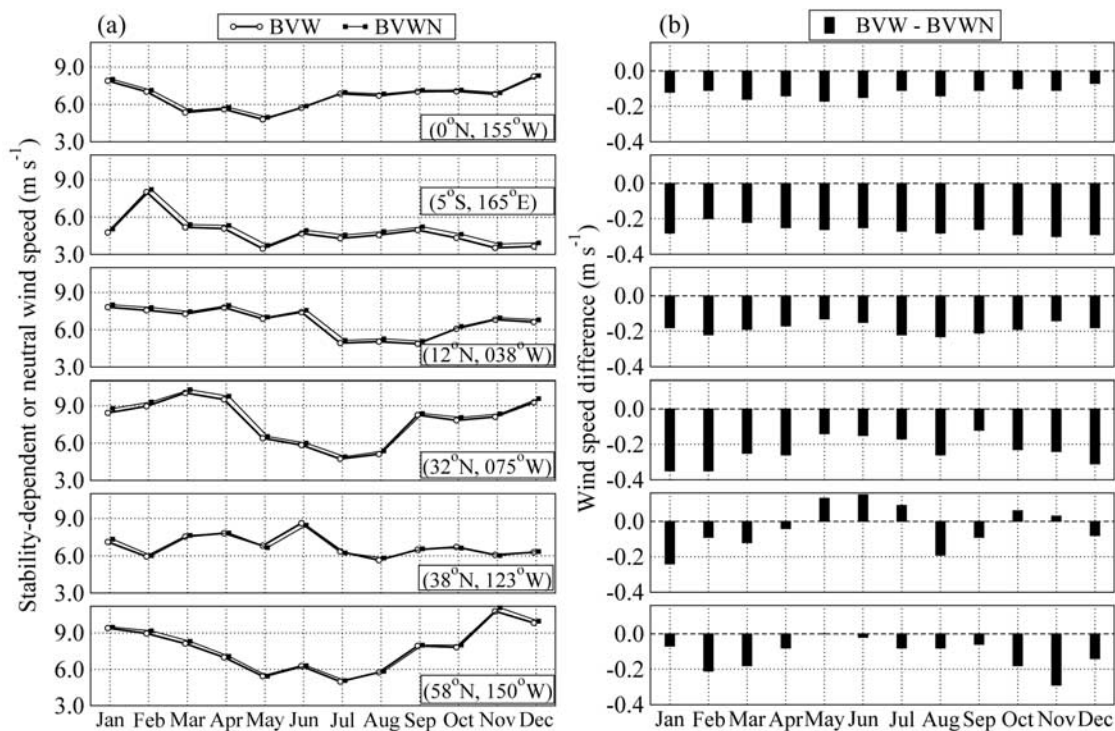


Figure 8. (a) Time series of monthly mean stability-dependent wind speed values and equivalent neutral wind speeds, both adjusted to 10 m, from various places over the global ocean in 2005. Monthly means were formed on the basis of daily averages at each buoy location. (b) Differences in stability-dependent and equivalent neutral wind speeds shown in Figure 8a.

values within the box are not equidistant from the hinges for BVW minus BVWN and BVW minus LKB during most of the month. Thus, wind speed differences are skewed. In the case of BVW minus LOG, median values are very close to the 5th percentiles. Overall, median difference values are not even the same between BVW minus BVWN and BVW minus LKB, but they are very close to each other (within 0.1 m s^{-1}) during most months. This indicates that LKB and BVWN generally provide identical equivalent neutral wind speeds even though they have different physical parameterizations.

[32] To give a further idea about monthly differences between stability-dependent and neutral winds, more examples are provided in Figure 8 for a given specific year, 2005. These locations are chosen at different places of the global ocean so that we can examine whether or not differences can be quite variable from one location to another since the stability conditions may vary depending on the region. These six particular buoys and their locations are as follows: (0°N , 155°W), a TAO buoy located in the central equatorial Pacific; (5°S , 165°E), a TAO buoy located in the western equatorial Pacific warm pool; (12°N , 38°W), a PIRATA buoy located in the Atlantic; (32°N , 75°W), a NDBC buoy, whose station ID is 41002, located in the east of Charleston, South Carolina, United States; (38°N , 123°W), a NDBC buoy, whose station ID is 46013, located north-northwest of San Francisco, California, United States; and (58°N , 150°W), a NDBC buoy, whose station ID is 46080, located in the Alaskan coast.

[33] At all buoy locations we first adjust hourly wind speeds to 10 m using BVW, and daily means are formed. Equivalent neutral winds are computed with BVWN. The conversion to 10 m buoy winds was made only when daily averaged ocean surface temperature, air temperature, and relative humidity were available from the buoy measurements. Otherwise that record was skipped. Monthly means were formed when all these essential variables from buoys were available at least 20 d. On the basis of some tests, a 20-d time period is found to be sufficient to represent monthly mean.

[34] Figure 8a shows that the annual cycles of equivalent neutral winds and winds including the effects of air-sea stability are typically similar. Equivalent neutral winds are always stronger in all months during 2005 except at (38°N , 123°W), where the stability conditions can result in weaker equivalent winds in May, June, July, October, and November (Figure 8b). Values of BVW minus BVWN are typically between 0 and -0.3 m s^{-1} .

[35] Finally, we would like to examine whether or not the differences between two wind types presented at six buoy locations are typically robust at other buoy locations (see Figure 2). Thus, a similar procedure for calculating stability-dependent and equivalent winds at those six sample buoy locations (see Figure 8a) is also performed at all TAO, NDBC, and PIRATA buoys from 2000 through 2005. A scatter diagram reveals that there are no systematic differences between the two (Figure 9a) when winds are adjusted to 10 m using BVW and equivalent winds are calculated

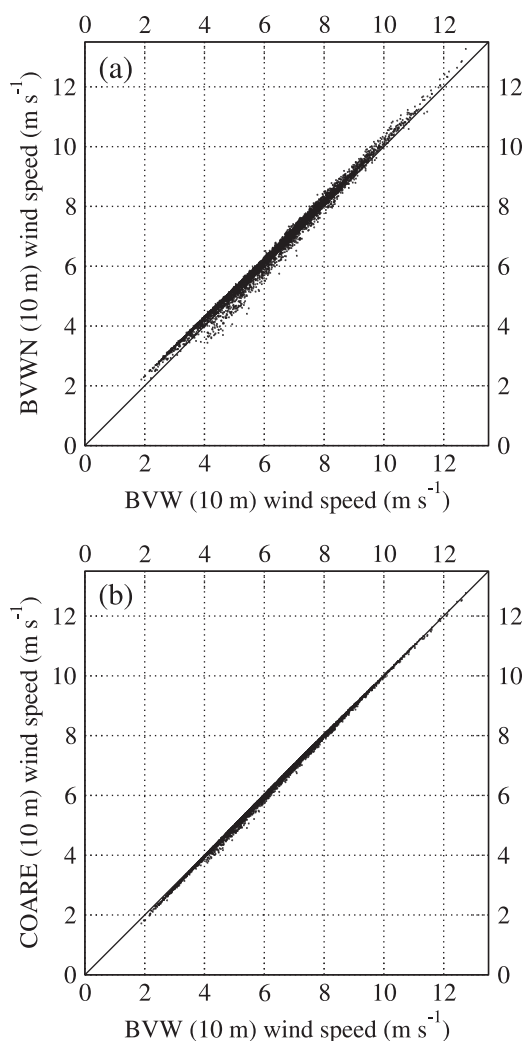


Figure 9. (a) A comparison of monthly mean equivalent neutral versus stability-dependent wind speed based on all buoys (NDBC, TAO, and PIRATA) during 2000–2005. Wind speeds at 10 m are calculated on the basis of BVW and BVWN using daily wind speed values at each buoy location. Average of all 7619 monthly mean stability-dependent (equivalent) winds is 6.3 m s^{-1} (6.5 m s^{-1}). (b) A comparison of BVW versus COARE algorithm based on wind speeds adjusted to 10 m by including the effects of stratification. As in Figure 9a, monthly mean wind speeds from all buoys are used. Average of all 7619 monthly mean stability-dependent wind speeds adjusted to 10 m using BVW (COARE) from all buoys is 6.3 m s^{-1} (6.3 m s^{-1}).

using BVWN. If one had adjusted winds to 10 m using COARE instead of BVW, the same results would have been obtained (Figure 9b), indicating that the use of either one of the algorithms in adjusting winds does not change results even when analyzing results at all buoy locations. This also confirms the consistency of BVW and COARE in adjusting winds to 10 m.

[36] Overall, on the basis of 7619 monthly mean wind speed values at all buoy locations during 2000–2005, neutral winds are stronger by 0.2 m s^{-1} than stability-dependent winds (Figure 9a). As to wind speed adjustment to 10 m performed

at all buoy locations during 2000–2005, BVW and COARE yield identical results with no (i.e., 0 m s^{-1}) wind speed bias (Figure 9a). This also explains that although both BVW and COARE essentially involve different physical approaches (see section 2), the resulting winds adjusted to 10 m are nearly identical. Thus, either one of the algorithms can be safely used for the adjustment process. Furthermore, we found no clear relationship between stability-dependent winds and differences between stability-dependent and equivalent neutral winds (Figure 10). There is a great deal of scatter from a wind speed–dependent trend. Thus, at a given location, it is not trivial to estimate the difference between the two by using either stability-dependent or equivalent neutral winds.

5.2. Differences Over the Global Ocean

[37] We now examine differences between stability-dependent and equivalent neutral winds over the global ocean. This will be accomplished using wind velocity measurements from the SeaWinds scatterometer on the QuikSCAT satellite. Hereinafter, they will be referred to as QSCAT winds. QSCAT measurements provide an excellent opportunity to examine stability-dependent and equivalent neutral wind difference because (1) they are calibrated to the neutral stability conditions, thus representing equivalent neutral winds, and (2) they can be converted to stability-dependent winds using air-sea stability. Both of these features will be described in this section in detail.

[38] Spaceborne radars (scatterometers) infer surface winds from the roughness of the ocean surface [e.g., Liu, 2002]. The scatterometer is an active microwave sensor that

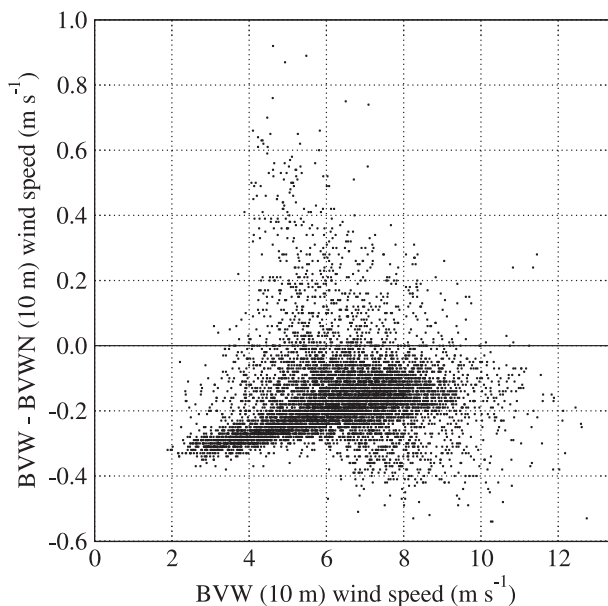


Figure 10. Scatterplot of differences between stability-dependent and equivalent neutral 10 m wind speeds with respect to the height-adjusted stability-dependent winds. This plot indicates that a wind speed–based parameterization cannot be used to approximate the differences between stability-dependent and equivalent neutral winds. Note also that most low wind speeds are associated with stable stratification and that the influence of stratification decreases as wind speed increases.

samples $\approx 90\%$ of the ice-free ocean in 1 d, most cells having a maximum of two observations per $25 \times 25 \text{ km}^2$ grid cell each day. However, there is a latitudinal dependence on sampling, with a greater average at higher latitudes. Measurements of radar backscatter from a given location on the ocean surface are obtained from multiple azimuth angles as the satellite travels along its orbit. These observations are acquired for two polarizations at different fixed incidence angles. Wind speed and direction are then inferred from measurement of microwave backscattered power from these multiple look angles. QSCAT was designed to measure ocean wind vectors with the accuracy requirement of root-mean-square of $\approx 2 \text{ m s}^{-1}$ for the wind range of $3\text{--}20 \text{ m s}^{-1}$. These requirements are essentially specified for a cell resolution of 25 km ($\approx 0.25^\circ$).

[39] Remote Sensing Systems provides twice-daily $0.25^\circ \times 0.25^\circ$ fields of equivalent neutral winds, available online at <http://www.remss.com>. To include stability effect for these winds, we first interpolated daily averaged sea-only fields (air temperature, humidity, etc.), obtained from the $1.125^\circ \times 1.125^\circ$ resolution European Centre for Medium-Range Weather Forecasts 40-year reanalysis (ERA-40), described by *Källberg et al.* [2004], to the $0.25^\circ \times 0.25^\circ$ QSCAT grid. We then use these with the BVW model to convert rain-free equivalent neutral winds to stability-dependent winds. ERA-40 is used when available (up to August 2002), and the $1.0^\circ \times 1.0^\circ$ Navy Operational Global Atmospheric Prediction System is used afterward (August 2002 through December 2005). Note that sea-only ERA-40 fields were produced by only using ocean points (based on the land-sea mask, set to 0.5 in the case of ERA-40's fractional mask), with creep-fill interpolation to cover land. *Kara et al.* [2007b] provide details of such interpolation to construct sea-only fields.

[40] The process of forming monthly winds is identical for equivalent and stability-dependent winds. In our processing, only twice-daily rain-free wind measurements from QSCAT are used over the global ocean. First, we form monthly averages on the $0.25^\circ \times 0.25^\circ$ grid using a cutoff of 20 rain-free observations per month. Then, from this we produce a 25-point (1.25° square) observation-weighted average at each 0.25° cell using a cutoff of 100 rain-free observations per month. Finally, we fill in all data voids (land- and rain-contaminated cells) using creep-fill interpolation [*Kara et al.*, 2007b]. This gives us a data set on a 0.25° grid with about the same effective resolution as ERA-40 ($1.125^\circ \times 1.125^\circ$).

[41] As an example, monthly means of equivalent neutral winds processed from QSCAT measurements are plotted in Figure 11a over the global ocean during January 2001. Note that there are no QSCAT wind observations above ice; thus, regions where ice is present (e.g., very high northern and southern latitudes) are masked and shown in gray. The ice-free regions are determined from an ice-land mask [*Reynolds et al.*, 2002]. The mask is a function of the ice analysis and changes by month. Equivalent neutral winds from QSCAT are then converted to winds that include stability effects, as seen in Figure 11a (middle).

[42] The conversion is accomplished using 6-hourly near-surface atmospheric variables (sea surface temperature, air temperature, and relative humidity) obtained from ERA-40. For the atmospheric variables, we first formed the 6-hourly

fields over the global ocean during January 2001 and then took a daily running mean once a day. The same process was also applied to other months. Spatial variations of the resulting stability-dependent winds are generally similar to those of equivalent neutral winds. This is also true for the magnitude of winds. In fact, the difference between the two is very small over most of the global ocean, as evident in Figure 11a (bottom).

[43] Similar to fields produced during January 2001, we also form monthly mean of winds during July 2001 (Figure 11b). Again, near-surface atmospheric variables from ERA-40 are used for determining the impact of air-sea stratification on winds. Seasonal variation in wind speeds is clear. For example, unlike January 2001, relatively strong winds are not seen at the North Atlantic and North Pacific oceans during July 2001. In fact, mean monthly winds are generally as low as $\approx 7 \text{ m s}^{-1}$ in these regions. Spatial variation of the difference field between the two wind types is also quite different (Figure 11b), although stability-dependent winds are again typically weaker than the neutral winds except at very high northern latitudes. Neutral winds being stronger by $>0.4 \text{ m s}^{-1}$ is also possible in the northernmost Atlantic and Pacific oceans. As in January 2001, the global average of the wind speed difference is very small, with a value of -0.07 m s^{-1} during July 2001, but spatial variability in the difference values must be noted.

[44] An investigation of the differences between the two wind speeds shown for the months of January and July in 2001 is extended to other months in the same year (Figure 12). The common feature seen in all plots is that stability-dependent winds are generally weaker than equivalent neutral winds over most of the global ocean. However, these differences are very small since neutral winds are typically stronger by 0.1 m s^{-1} than stability-dependent winds. Spatial patterns of the differences are generally similar, but some deviations arise in some regions, indicating the relatively large impact of air-sea stability.

[45] In Figure 12, differences between the two wind types are examined only during 2001. Are differences between the two similar for other years? To answer this question, we processed QSCAT winds during 2000 and 2002. Equivalent neutral winds were converted to stability-dependent winds using near-surface atmospheric variables from ERA-40 as in 2001. Figure 13 shows differences between stability-dependent and neutral wind speeds. The resulting differences are again small; however, there are regional interannual differences that might be important.

6. Application of Stability-Dependent Versus Neutral Winds

[46] In section 5.2, we found that stability-dependent and equivalent neutral winds are typically similar to each other over most of the global ocean. Monthly mean differences are generally within $\approx 0.2 \text{ m s}^{-1}$. We also suggested that stability considerations can lead to important differences in wind speed on short timescales, while the main global results are presented as monthly averages only. In this section, the importance of air-sea stability effects on 10 m winds is further explored with an application involving heat fluxes over the global ocean on shorter timescales.

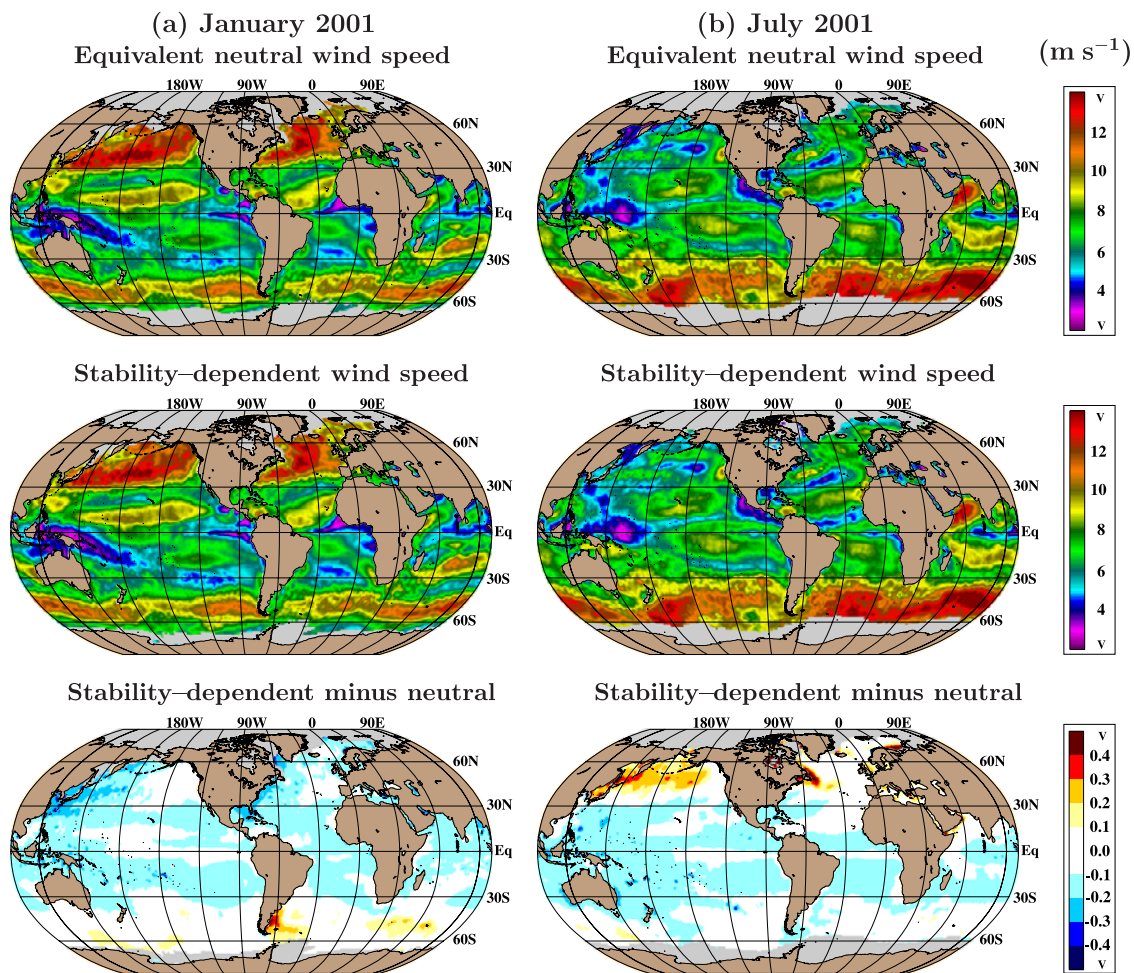


Figure 11. Comparisons of monthly mean equivalent neutral wind speed and stability-dependent wind speed (both are at 10 m above the sea surface) constructed from rain-free QSCAT measurements over the global ocean: (a) January 2001 and (b) July 2001. Note that monthly means were constructed from daily fields.

[47] Our main goal is to answer how air-sea heat fluxes would change if one used equivalent neutral winds, which are directly obtained from the satellite, instead of stability-dependent winds. As an example, equivalent neutral winds from QSCAT winds are obtained at the first pass of the satellite over the global ocean on 1 January and 1 August 2002. They are then converted to stability-dependent winds on the basis of the BVW algorithm. Unlike the monthly analyses, differences between stability-dependent and equivalent neutral winds are slightly higher (Figure 14). However, the largest stability effects occur in ocean regions that are characterized by either western boundary currents or meander regions of the Antarctic Circumpolar Current (i.e., the Southern Ocean regions) as noted in the monthly mean fields.

[48] Given those differences in stability-dependent and equivalent neutral winds, sensible and latent heat fluxes are also computed on the basis of the bulk heat parameterizations in COARE (version 3.0) and near-surface atmospheric variables from ERA-40 at each ocean grid point. Heat fluxes are computed with two inputs separately: (1) stability-dependent winds and (2) equivalent neutral winds. Differences in fluxes

are formed by subtracting equivalent neutral winds from stability-dependent winds. The resulting sensible and latent heat flux differences are generally negligible (Figure 14). Sensible (latent) heat flux differences are within 1 W m^{-2} (2 W m^{-2}) over most of the global ocean.

[49] Including the impact of air-sea stability causes relatively large effects on heat fluxes only near the Gulf Stream and Kuroshio current systems on 1 January 2002 (Figure 14a). These are the regions where winds and magnitude of latent heat fluxes are relatively large in comparison to other regions (not shown), resulting in large differences. Stratification effects on winds are even smaller, as evident from the heat flux difference fields on 1 August 2002 (Figure 14b). No significant spatial variations are noted during either time period. Overall, in isolated regions associated with large air-sea temperature and specific humidity differences (and typically ocean fronts), we find that the adjusted surface turbulent fluxes differ by over 5 W m^{-2} , which is considered significant as a short- to medium-term bias [Webster and Lukas, 1992]. These biases vary seasonally, but within such regions they are often significant as judged by this standard. Other work in

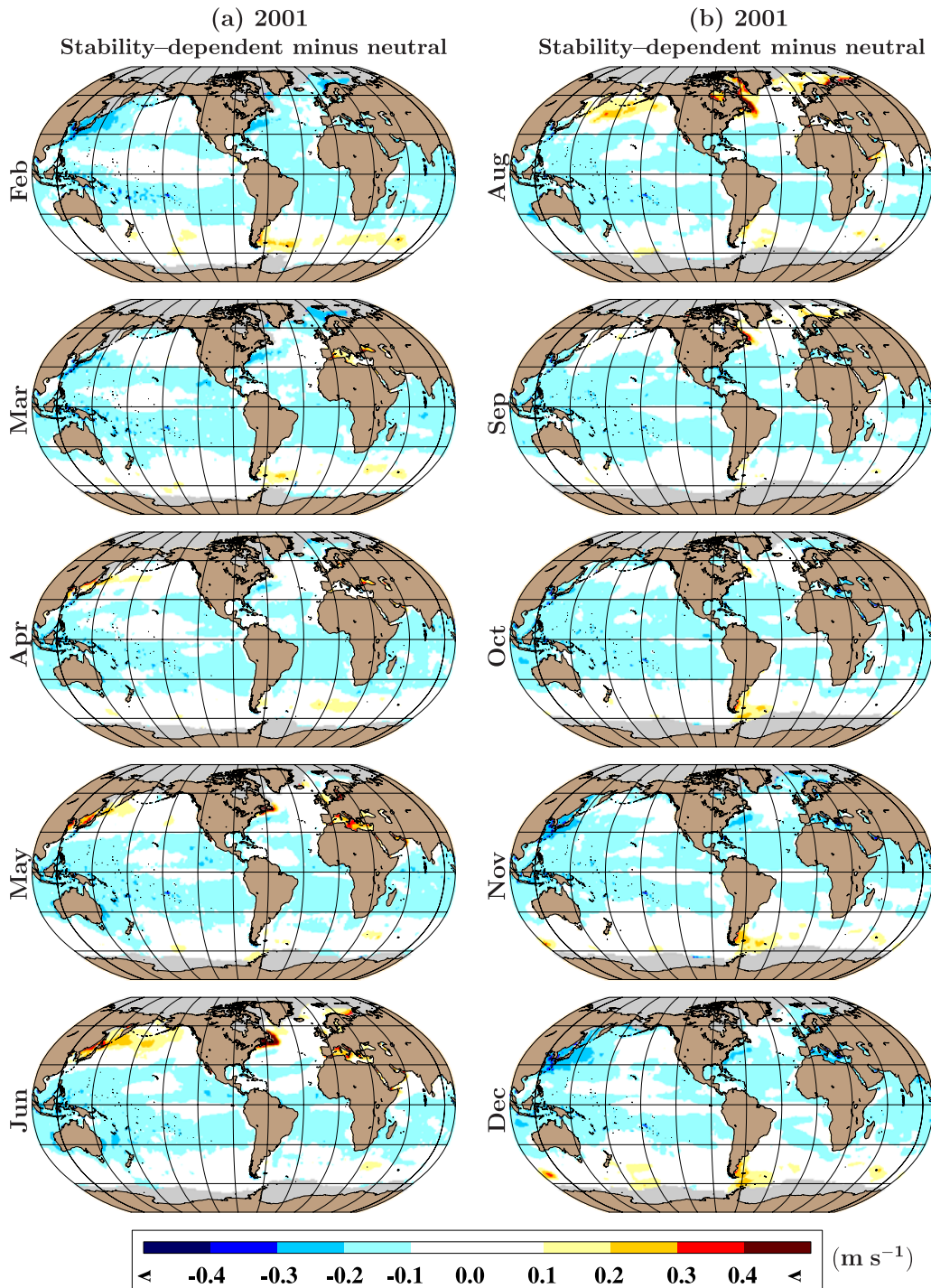


Figure 12. Differences in monthly mean 10 m wind speed (a) from February through June 2001 and (b) from August through December 2001. Differences in January and July are given in Figure 11. Blue (red) denotes regions where stability-dependent wind speed is weaker (stronger) than equivalent neutral wind speeds.

progress shows that there are large monthly biases in these regions.

7. Conclusions

[50] Important physical processes (e.g., surface fluxes, wave evolution, and in some cases upper ocean mixing) are

typically parameterized in terms of wind speed or stress inferred from wind speed. For historical reasons, wind speeds are used rather than equivalent neutral wind speeds, which are typically available from satellites. A quantitative analysis of differences between the two wind types is desired to determine possible errors (particularly biases) due to improper use of equivalent neutral winds.

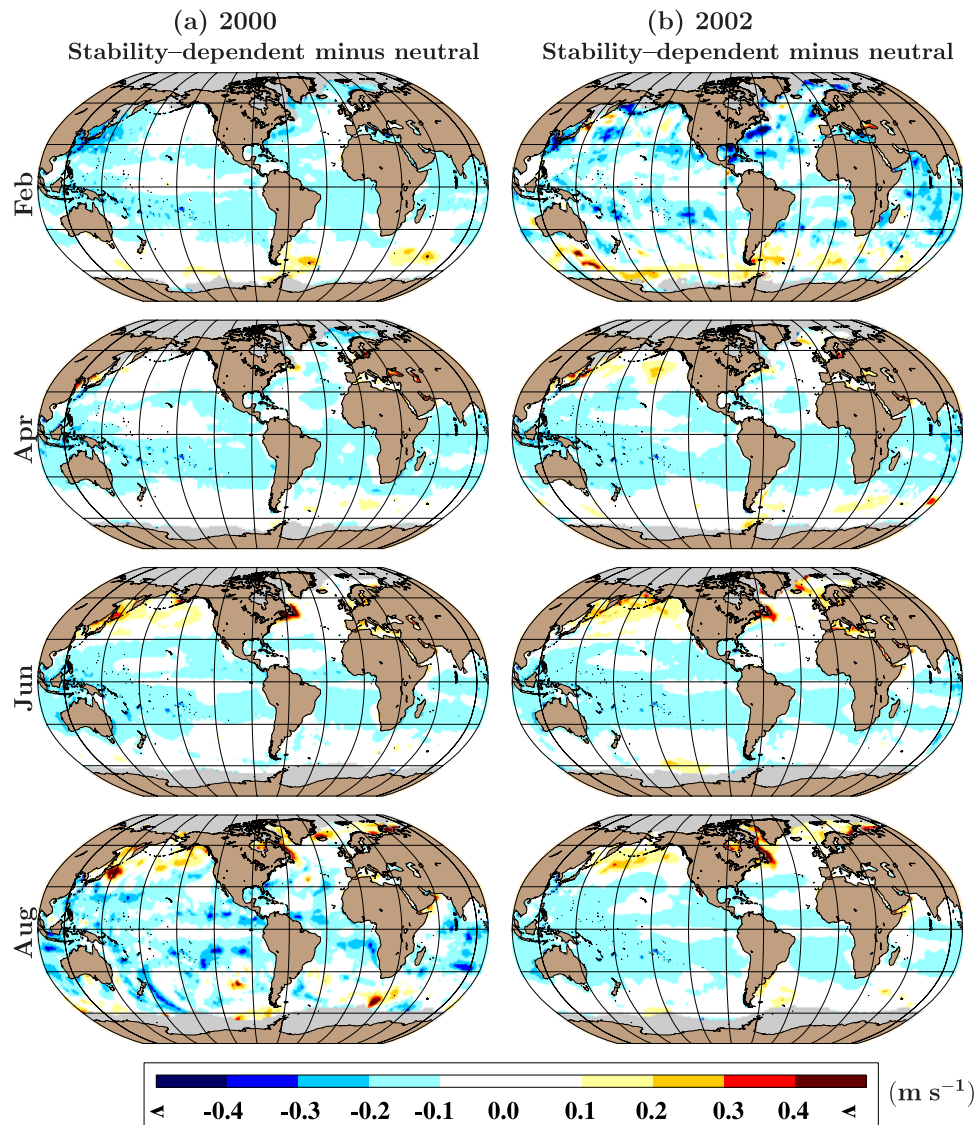


Figure 13. Differences in monthly mean 10 m wind speed during February, April, June, and August of (a) 2000 and (b) 2002.

[51] Stability-related differences between winds and equivalent neutral winds are found to be small on monthly timescales. However, sampling is sufficient that the small signal is easily identified. When scatterometer winds are used for the calculation of surface turbulent fluxes or surface wave models or for product validation, they are large enough to contribute to physically noticeable differences. The distribution of the differences between the stability-dependent winds and equivalent neutral winds, combined with the number of samples that go into forming an average value, reveals typical magnitudes of biases in using equivalent neutral winds as a proxy for stability-dependent winds. These biases are larger on short timescales (e.g., hourly) for which there can be greater departures from neutral stability and limited sampling of independent environmental condition. Furthermore, conversion of equivalent neutral winds to stability-dependent winds should be performed with a technique that considers the dependence of

surface roughness on stress. A simple log law adjustment using a fixed roughness length typically estimates relatively small corrections with the incorrect sign. The LKB and BVW flux models have very different physical considerations; however, both include a feedback between stability and roughness length. The differences in adjustment between these two models are negligible, typically within $\pm 0.1 \text{ m s}^{-1}$, which is substantially smaller than most adjustments.

[52] Wide-ranging applications of QSCAT winds would benefit from the conversion of equivalent neutral winds to stability-dependent winds which are used for computing wind stresses. For example, winds are generally weaker than the neutral winds by $\pm 0.2 \text{ m s}^{-1}$ over the global ocean, but differences between the two can even be up to $\pm 0.5 \text{ m s}^{-1}$ at high latitudes on a monthly timescale and much larger on a shorter timescale (e.g., daily). For comparisons between QSCAT winds and model or buoy winds, on a shorter scale

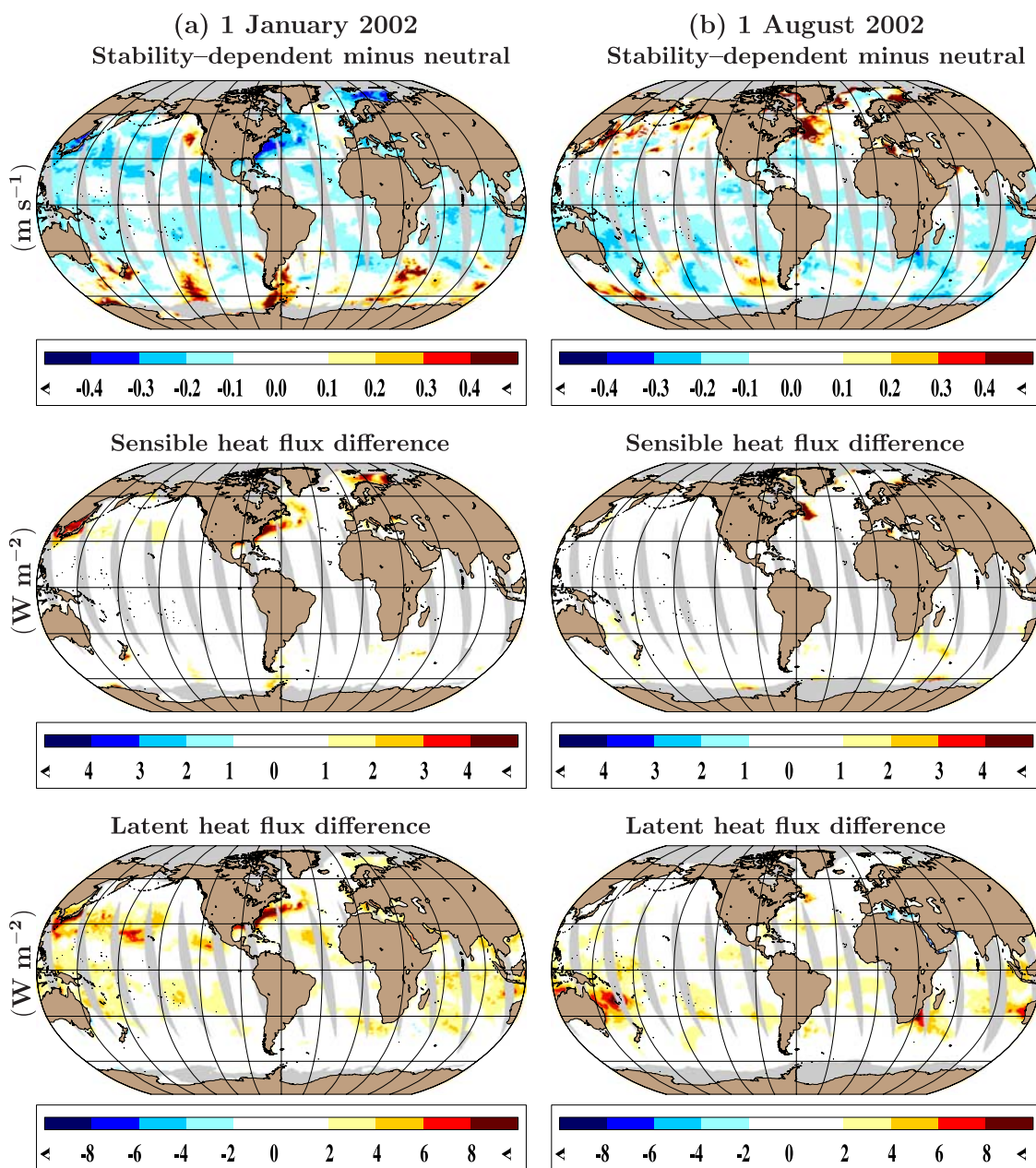


Figure 14. (a) Differences in 10 m wind speed and sensible and latent heat fluxes during the first satellite pass on 1 January 2002. Differences in heat fluxes are computed using stability-dependent and equivalent neutral winds in the COARE (version 3.0) algorithm as explained in the text. (b) The same as Figure 14a but during the first satellite pass on 1 August 2002.

(e.g., hourly or daily), there are likely to be sufficient observations that ignoring this adjustment will result in a statistically and physically significant bias. Our previous work has also revealed that biases due to ocean current and wave motions can be regionally important [Kara *et al.*, 2007a].

[53] For potential users of interest, hourly and daily wind speeds (both stability-dependent and neutral ones) and other near-surface atmospheric variables adjusted to 10 m using historical data (1980 through 2005) from all TAO, NDBC, and PIRATA buoys are available (<http://www7320.nrlssc.navy.mil/nasec>). The adjustment is made using all air-sea flux algorithms (COARE, LKB, BVW, BVWN, and LOG) dis-

cussed in this paper. Rain-free QSCAT winds are also available over the global ocean.

[54] **Acknowledgments.** This work is funded by the Office of Naval Research (ONR) under the 6.1 project Global Remote Littoral Forcing via Deep Water Pathways. M. A. Bourassa's research is funded through the NASA OVVST. QSCAT wind measurements are produced by RSS. The paper is contribution NRL/JA/7320/07/7092 and has been approved for public release. Much appreciation is extended to the reviewers whose helpful comments improved the quality of this paper. We would like to thank D. Smith of RSS for numerous discussions.

References

Barron, C. N., A. B. Kara, P. J. Martin, R. C. Rhodes, and L. F. Smedstad (2006), Description and application of the global Navy Coastal Ocean

- Model (NCOM) with examination of vertical coordinate system choices, *Ocean Modell.*, *11*, 347–375.
- Beljaars, A. C. M., and A. A. M. Holtslag (1991), Flux parameterization over land surfaces for atmospheric models, *J. Appl. Meteorol.*, *30*, 327–341.
- Benoit, R. (1977), On the integral of the surface layer profile-gradient functions, *J. Appl. Meteorol.*, *16*, 859–860.
- Bourassa, M. A. (2006), Satellite-based observations of surface turbulent stress during severe weather, in *Atmosphere-Ocean Interactions*, vol. 2, edited by W. Perrie, pp. 35–52, Wessex Inst. of Technol., Southampton, UK.
- Bourassa, M. A., D. G. Vincent, and W. L. Wood (1999), A flux parameterization including the effects of capillary waves and sea state, *J. Atmos. Sci.*, *56*, 1123–1139.
- Bourassa, M. A., D. M. Legler, J. J. O'Brien, and S. R. Smith (2003), SeaWinds validation with research vessels, *J. Geophys. Res.*, *108*(C2), 3019, doi:10.1029/2001JC001028.
- Brunke, M. A., C. W. Fairall, X. Zeng, L. Eymard, C. Laurence, and J. A. Cury (2003), Which bulk aerodynamic algorithms are least problematic in computing ocean surface turbulent fluxes?, *J. Clim.*, *16*, 619–635.
- Chelton, D. B., M. G. Schlax, M. H. Freilich, and R. F. Milliff (2004), Satellite measurements reveal persistent small-scale features in ocean winds, *Science*, *303*, 978–983.
- Ebuchi, N., H. C. Graber, and M. J. Caruso (2002), Evaluation of wind vectors observed by QuikSCAT/SeaWinds using ocean buoy data, *J. Atmos. Oceanic Technol.*, *19*, 2049–2062.
- Fairall, C. W., E. F. Bradley, J. E. Hare, A. A. Grachev, and J. B. Edson (2003), Bulk parameterization of air-sea fluxes: Updates and verification for the COARE algorithm, *J. Clim.*, *16*, 571–591.
- Freitag, H. P., M. O'Haleck, G. C. Thomas, and M. J. McPhaden (2001), Calibration procedures and instrumental accuracies for ATLAS wind measurements, *NOAA Tech. Memo. OAR PMEL-119*, 20 pp., Pac. Mar. Environ. Lab., NOAA, Seattle, Wash.
- Geernaert, G. L., and K. B. Katsaros (1986), Incorporation of stratification effects on the oceanic roughness length in the derivation of the neutral drag coefficient, *J. Phys. Oceanogr.*, *16*, 1580–1584.
- Gierach, M. M., M. A. Bourassa, P. Cunningham, P. Reasor, and J. J. O'Brien (2007), Vorticity-based detection of tropical cyclogenesis, *J. Appl. Meteorol. Climatol.*, *46*, 1214–1229.
- Grachev, A. A., C. W. Fairall, and E. F. Bradley (2000), Convective profile constants revisited, *Boundary Layer Meteorol.*, *94*, 495–515.
- Grachev, A. A., C. W. Fairall, P. O. G. Persson, E. L. Andreas, and P. S. Guest (2005), Stable boundary-layer scaling regimes: The SHEBA data, *Boundary Layer Meteorol.*, *116*, 201–235.
- Källberg, P., A. Simmons, S. Uppala, and M. Fuentes (2004), The ERA-40 archive, *ERA-40 Proj. Rep. Ser.*, *17*, 31 pp., Eur. Cent. for Medium-Range Weather Forecasts, Reading, UK.
- Kara, A. B., H. E. Hurlburt, and A. J. Wallcraft (2005), Stability-dependent exchange coefficients for air-sea fluxes, *J. Atmos. Oceanic Technol.*, *22*, 1080–1094.
- Kara, A. B., E. J. Metzger, and M. A. Bourassa (2007a), Ocean current and wave effects on wind stress drag coefficient over the global ocean, *Geophys. Res. Lett.*, *34*, L01604, doi:10.1029/2006GL027849.
- Kara, A. B., A. J. Wallcraft, and H. E. Hurlburt (2007b), A correction for land contamination of atmospheric variables near land-sea boundaries, *J. Phys. Oceanogr.*, *37*, 803–818.
- Lagerloef, G. S. E., R. Lukas, F. Bonjean, J. T. Gunn, G. T. Mitchum, M. A. Bourassa, and A. J. Busalacchi (2003), El Niño tropical Pacific Ocean surface current and temperature evolution in 2002 and outlook for early 2003, *Geophys. Res. Lett.*, *30*(10), 1514, doi:10.1029/2003GL017096.
- Liu, W. T. (2002), Progress in scatterometer application, *J. Oceanogr.*, *58*, 121–136.
- Liu, W. T., and W. Tang (1996), Equivalent neutral wind, *JPL Publ.*, *96-17*, 8 pp.
- McPhaden, M. J., et al. (1998), The Tropical Ocean–Global Atmosphere observing system: A decade of progress, *J. Geophys. Res.*, *103*, 14,169–14,240.
- Mears, C. A., D. K. Smith, and F. J. Wentz (2001), Comparison of Special Sensor Microwave Imager and buoy-measured wind speeds from 1987 to 1997, *J. Geophys. Res.*, *106*, 11,719–11,729.
- Meissner, T., D. Smith, and F. Wentz (2001), A 10 year intercomparison between collocated Special Sensor Microwave Imager oceanic surface wind speed retrievals and global analyses, *J. Geophys. Res.*, *106*, 11,731–11,742.
- Peixoto, J. P., and A. H. Oort (1992), *Physics of Climate*, 520 pp., Am. Inst. of Phys., Woodbury, N. Y.
- Reynolds, R. W., N. A. Rayner, T. M. Smith, D. C. Stokes, and W. Wang (2002), An improved in situ and satellite SST analysis for climate, *J. Clim.*, *15*, 1609–1625.
- Ross, D. B., V. J. Cardone, J. Overland, R. D. McPherson, W. J. Pierson Jr., and T. Yu (1985), Oceanic surface winds, *Adv. Geophys.*, *27*, 101–138.
- Servain, J., A. J. Busalacchi, M. J. McPhaden, A. D. Moura, G. Reverdin, M. Vianna, and S. E. Zebiak (1998), A Pilot Research Moored Array in the Tropical Atlantic (PIRATA), *Bull. Am. Meteorol. Soc.*, *79*, 2019–2031.
- Webster, P. J., and R. Lukas (1992), TOGA-COARE: The Coupled Ocean-Atmosphere Response Experiment, *Bull. Am. Meteorol. Soc.*, *73*, 1377–1416.
- Weissman, D. E., K. L. Davidson, R. A. Brown, C. A. Friehe, and F. Li (1994), The relationship between the microwave radar cross section and both wind speed and stress: Model function studies using Frontal Air-Sea Interaction Experiment data, *J. Geophys. Res.*, *99*, 10,087–10,108.

M. A. Bourassa, Center for Ocean-Atmospheric Prediction Studies, Florida State University, Tallahassee, FL 32306, USA.

A. B. Kara and A. J. Wallcraft, Oceanography Division, Naval Research Laboratory, Code 7320, Building 1009, Stennis Space Center, MS 39529, USA. (birol.kara@nrlssc.navy.mil)